Improved Seismic Collapse Prediction of Inelastic Simple Systems Vulnerable to the P-delta Effect Based on Average Spectral Acceleration

S. Tsantaki, C. Jäger & C. Adam
University of Innsbruck, Department of Civil Engineering Sciences, Austria

SUMMARY:
In this paper the prediction of the collapse capacity of single-degree-of-freedom (SDOF) systems vulnerable to the P-delta under severe earthquake excitation is improved in the sense that its dispersion due to record-to-record variability is reduced. Recently, two of the authors have introduced the concept of so-called collapse capacity spectra. In the original study, the 5% damped spectral acceleration at the structural period serves as intensity measure (IM) of the seismic excitation. However, this definition of the IM leads to a quite large dispersion of the collapse capacity. Alternatively, in the present study an average spectral acceleration over a range of periods serves as IM, thus taking into account the period elongation of inelastic SDOF systems. Consequently, the collapse capacity dispersion decreases significantly by at least 25%.

Keywords: collapse capacity; dispersion; intensity measure; P-delta effect; record-to-record variability

1. INTRODUCTION

The first generation of performance-based earthquake engineering (PBEE) methodologies (FEMA 273 1997, ATC 40 1996) is based on forces and deformations as structural response indices, and on prescriptive performance levels. These methodologies are largely deterministic apart from the probabilistic definition of the seismic hazard (Deierlein 2004). The next generation of PBEE procedures (ATC 58 2009 and FEMA P-695 2009) with a rigorous probabilistic framework transposes the inherent uncertainties into the whole process of performance-based assessment. In earthquake engineering these uncertainties are divided into two categories: Aleatory uncertainties due to natural randomness such as record-to-record and spatial variability, and epistemic uncertainties due to parametric and model variability.

The present study aims at reducing the record-to-record variability when predicting collapse and the collapse fragility of inelastic single-degree-of-freedom (SDOF) systems sensitive to the second-order effects of gravity (P-delta effect). Fundamental studies of P-delta effect on inelastic SDOF systems subjected to earthquakes have been presented in Bernal (1987) and MacRae (1994). Asimakopoulos et al. (2007) propose a simple formula for a yield displacement amplification factor as a function of the ductility and the stability coefficient. Miranda and Akkar (2003) present an empirical equation to estimate the minimum lateral strength up to which P-delta induced collapse of SDOF systems is prevented. In Adam and Jäger (2012a, b) so-called collapse capacity spectra have been introduced for the seismic collapse assessment of SDOF structures with non-degrading structural properties.

One objective of this study is the investigation of the influence of a proposed intensity measure (IM) on the record-to-record randomness by conducting extensive Incremental Dynamic Analyses (IDAs) (Vamvatsikos and Cornell 2002) on SDOF systems vulnerable to the P-delta effect, at which material degradation is assumed to be negligible. Consequently, collapse capacity spectra (Adam and Jäger 2012a) are improved, providing a compact, accurate and easily applicable tool for practising engineers. In the original study (Adam and Jäger 2012a), which is the benchmark for this research, the IM used is the ratio of 5% damped spectral acceleration at the structural period to the base shear

coefficient. However, this definition of the IM leads to a quite large dispersion of the collapse capacity. Thus, following an idea of Bianchini et al. (2009) the mean spectral acceleration over a range of periods is employed, taking into consideration the period elongation of inelastic SDOF systems. In this period range the structure's period serves as the lower limit.

2. DEFINITIONS AND FRAMEWORK

2.1. The P-Delta Effect on an Inelastic SDOF System

In an inelastic SDOF system the gravity load generates a shear deformation of its hysteretic force-displacement relationship. Characteristic displacements (such as the yield displacement) of this relationship remain unchanged, whereas the characteristic forces (such as the strength) are reduced. As a result, the slope of the curve is decreased in its elastic and post-elastic branch of deformation. The magnitude of this reduction can be expressed by means of the so-called stability coefficient θ (MacRae 1994). θ is a function of the gravity load, geometry, and stiffness. As a showcase Fig. 2.1 visualizes the P-delta effect on the hysteretic behaviour of a SDOF system with non-deteriorating bilinear characteristics. In this example the post-yield stiffness is negative, because the stability coefficient θ is larger than the hardening ratio α.

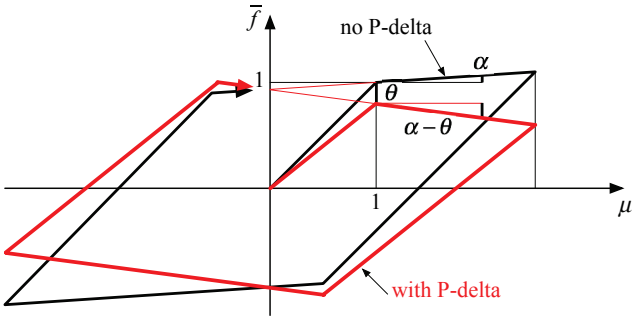

Figure 2.1. Normalized bilinear cyclic structural behaviour with and without the destabilizing effect of gravity loads (Adam and Jäger 2012a)

A negative slope of the post-tangential stiffness, expressed by the difference of the stability coefficient θ and the strength hardening coefficient α, $\theta-\alpha$, is the essential condition that the structure may collapse under severe earthquake excitation. In Adam and Jäger (2012a) it is shown that collapse of inelastic SDOF systems vulnerable to P-delta is mainly governed by the following parameters:

- The negative slope of the post-tangential stiffness $\theta-\alpha$,
- the elastic structural period of vibration T_1,
- the viscous damping coefficient ζ (usually taken as 5%), and
- the shape of the hysteretic loop.

2.2. Intensity Measure

There is no unique definition of intensity of an earthquake record. Consequently, several IMs have been proposed and used such as elastic ground motion based scalar IMs (e.g. peak ground acceleration (PGA), peak ground velocity (PGV), peak ground displacement (PGD) (Adam and Jäger 2012b)), elastic and inelastic spectral based IMs (e.g. spectral acceleration S_a and spectral displacement S_d, respectively, at the fundamental period T_1 of the structure: $S_a(T_1)$, $S_d(T_1)$ (Tothong and Luco 2007)), and vector valued IMs (e.g. $S_{a,\varepsilon}$, for details see Baker and Cornell (2005)). More recently, spectral IMs considering the period elongation of inelastic structures have been presented by Haselton and Baker (2006), Bianchini et al. (2009), and Kadas et al. (2011). However, the most widely used IM is currently the 5% damped spectral acceleration S_a at the fundamental period T_1 of the structure, $S_a(T_1)$.

The IM is the interface between seismology and engineering (Baker 2007). It quantifies the severity of a seismic event, and it is a scale factor for the IDA procedure. According to Bianchini et al. (2009) an appropriate IM must comply with the following properties, that is hazard compatibility, sufficiency, scaled robustness, and efficiency. Baker and Jayaram (2008) describe how ground motion prediction models (so-called attenuation relationships) can be developed for an averaged spectral acceleration over a period band ΔT. In this study, the definition of Bianchini et al. (2009) for an averaged spectral acceleration as the geometric mean of *n* 5% damped spectral pseudo-acceleration ordinates,

$$S_{a,av}(\beta T_1, T_e) = \sqrt[n]{S_a(\beta T_1) S_a(\beta T_1 + \delta T) S_a(\beta T_1 + 2\delta T) \ldots\ldots\ldots S_a(T_e = \beta T_1 + n\delta T)} \tag{2.1}$$

which satisfies the first of these properties, is utilized. Note that $\Delta T = n\delta T$. According to Eqn. 2.1 $S_{a,av}(\beta T_1, T_e)$ is the geometric mean of 5% damped spectral accelerations at discrete structural periods ranging from period βT_1 (with T_1 denoting the fundamental period) to the elongated period T_e. Note that coefficient $\beta\,(\leq 1)$ is introduced to account for higher mode effects. Bianchini et al. (2009) show that $S_{a,av}(\beta T_1, T_e)$ is statistically independent from ground motion characteristics and scaling factors, and thus it complies with the IM properties sufficiency and scaled robustness.

This study focuses on the investigation of efficiency of $S_{a,av}(T_1, T_e)$ with respect to the reduction of collapse capacity dispersion due to the record-to-record variability. Since this study concerns SDOF systems, subsequently the coefficient β is set equal to one ($\beta = 1.0$).

2.3. Ground Motion Scaling

In this study, the aleatory uncertainties are captured employing the 44 far-field ground motions of the ATC63-FF record set described in FEMA P-695 (2009). To obtain comparable results, the ground motion records must be scaled. When using Eqn. 2.1 as an IM, scaling of the original *i*th ground acceleration $\ddot{x}^{(i)}_{g,unscaled}$ must be performed over the period band $\Delta T = T_e - T_1$ to account for the spectral shape within ΔT according to

$$\ddot{x}^{(i)}_{g,scaled} = \frac{S^{ref}_{a,av}(T_1, T_e)}{S^{(i)}_{a,av}(T_1, T_e)} \ddot{x}^{(i)}_{g,unscaled} \tag{2.2}$$

Thereby, $S^{ref}_{a,av}(T_1, T_e)$ is the target value of the averaged spectral acceleration, which is the same value for all ground motions of the considered record set.

2.4. Collapse Capacity

The collapse capacity is defined as the maximum ground motion intensity at which the structure still maintains dynamic stability (Krawinkler et al. 2009). Most generally the IDA procedure is applied to predict the collapse capacity. In an IDA for a given structure and a given acceleration time history of an earthquake record dynamic time history analyses are performed repeatedly, where in each subsequent run the intensity of the ground motion is incremented. As an outcome a characteristic IM is plotted against the corresponding maximum characteristic structural response quantity for each analysis. The procedure is stopped, when the response grows to infinity, that is structural failure occurs. The corresponding IM is referred to as collapse capacity of the considered structure for this specific ground motion record (denoted by *i*). In this study the relative collapse capacity of the *i*th ground motion record corresponds to the suggested IM $S^{(i)}_{a,av}(T_1, T_e)$ at collapse divided by the base shear coefficient γ,

$$CC_i\big|_{S_{a,av}} = \frac{S^{(i)}_{a,av}(T_1, T_e)\big|_{collapse}}{g\gamma}, \qquad \gamma = \frac{f_y}{mg} \tag{2.3}$$

f_y is the yield strength and m the mass of the SDOF system, and g denotes the gravity. Since the inherent record-to-record variability leads to different collapse capacities for different ground motion records, the collapse capacities are determined for all records of a ground motion set, and subsequently evaluated statistically. Ibarra and Krawinkler (2005, 2011) provide good arguments for representing a set of corresponding collapse capacities by a log-normal distribution. A log-normal distribution is characterized by the median of the individual collapse capacities CC_i (referred to as CC), and the 16th and 84th percentiles of the collapse capacities denoted as CC_{16} and CC_{84}, respectively. In the following the dispersion quantity s^* (Adam and Jäger 2012a)

$$s^* = \ln\sqrt{s_u s_l} \quad , \; s_u = \frac{CC_{84}}{CC} \quad , \; s_l = \frac{CC}{CC_{16}} \tag{2.4}$$

is utilized as a representative measure of the variability of the individual collapse capacities. Note that in the log-domain s^* corresponds to the standard deviation, $\sigma \approx s^*$. For details see Limpert et al. (2001).

2.5. Collapse Capacity Spectrum

In a collapse capacity spectrum the representative collapse capacity of a P-delta sensitive and non-deteriorating SDOF system with given negative post-yield stiffness ratio $\theta - \alpha$, viscous damping ζ, and hysteretic loop is presented as a function of the structural period T_1 (Adam and Jäger 2012a). As an example, Fig. 2.2 shows 5% damped median collapse capacity spectra (black lines) in the period range from $T_1 = 0.1$ to $T_1 = 5$ s based on the conventional IM $S_a(T_1)$ for bilinear SDOF systems with various negative post-yield stiffness ratios $\theta - \alpha$. These spectra were derived by Adam and Jäger (2012a) using the records of the ATC63-FF ground motion set. The smooth curves in red represent the corresponding so-called design collapse capacity spectra as a result from non-linear regression analyses.

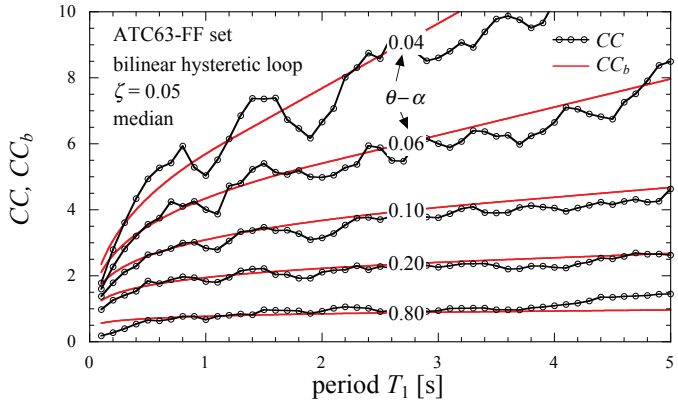

Figure 2.2. Median collapse capacity spectra CC and corresponding smooth design collapse capacity spectra CC_b based on the conventional IM $S_a(T_1)$ (Adam and Jäger 2012a)

3. DISPERSION OF THE COLLAPSE CAPACITY

3.1. Record-to-Record Variability for Various Intensity Measures

In an initial study the effect of the record-to-record variability on the collapse capacity is studied. Thereby, for one structural configuration (i.e. $\theta - \alpha = 0.30$, $\zeta = 0.05$, bilinear hysteretic loop) collapse capacities based on the originally used conventional IM $S_a(T_1)$ are set in contrast with outcomes based on the proposed IM $S_{a,av}(T_1,T_e)$. Initially, for the IM $S_{a,av}(T_1,T_e)$ a scaling band width of $\Delta T = 1.2$ s is selected "arbitrarily". The graphical representation of the derived record-to-

record variability of the evaluated collapse capacities is shown in Fig. 3.1. Thereby, the collapse capacities are plotted in the log-domain against several discrete values of the structural period T_1. The dispersion of the collapse capacity characterized by the 16th and 84th percentile values is marked by blue boxes. A red line represents the median of the collapse capacity. Additionally, thin black lines represent the smallest and largest collapse capacity, respectively. Comparing the results of the left and the right plot reveals that for systems with periods $T_1 > 0.5\,\text{s}$ the IM $S_{a,av}(T_1,T_e)$ is more efficient than the IM $S_a(T_1)$, because the dispersion of the collapse capacity is much smaller. In contrast, for short period systems ($T_1 = 0.1\,\text{s}, 0.5\,\text{s}$) the IM $S_a(T_1)$ leads to a smaller variability of the collapse capacities.

Fig. 3.2 shows the effect of the improved IM on the collapse fragility for a SDOF system with the parameters $T_1 = 0.70$ s and $\theta - \alpha = 0.30$. Collapse fragility curves incorporate explicitly the aleatory uncertainties due to record-to-record variance. Additionally to the sorted collapse capacities, a fit of these curves based on the assumption of a log-normal distribution is shown. For the proposed IM scaling period band width ΔT of 0.4 s, 0.8 s, and 1.2 s are taken into account. Blue lines represent the outcomes using the conventional IM $S_a(T_1)$ (i.e. $\Delta T = 0$). The reduction of the dispersion for the proposed IM $S_{a,av}(T_1,T_e)$ is obvious, because the collapse fragility curves become more vertical in comparison with the collapse fragility curve for $S_a(T_1)$. In this particular example problem the dispersion is smallest for the band width ΔT of 0.4 s. Additionally, it can be seen that the median collapse capacity is reduced with increasing ΔT.

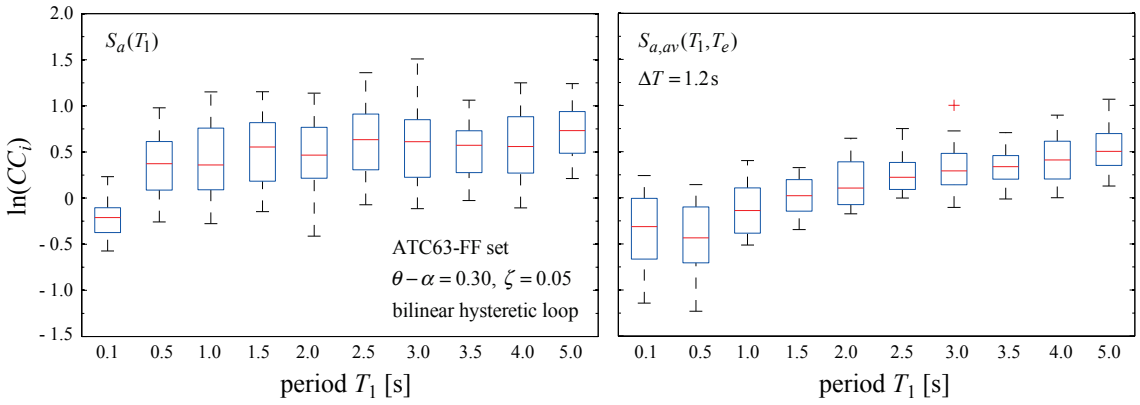

Figure 3.1. Box plots of the collapse capacities for different structural periods T_1 based (a) on the conventional IM $S_a(T_1)$, and (b) on the proposed IM $S_{a,av}(T_1,T_e)$ with $\Delta T = 1.2$ s

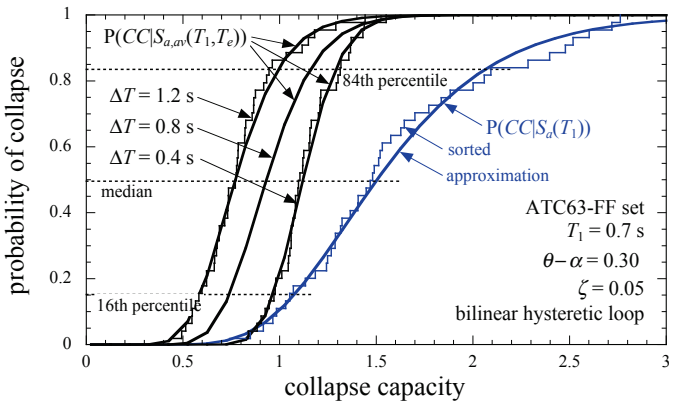

Figure 3.2. Collapse fragility curves for the conventional IM $S_a(T_1)$ (blue graphs), and for the proposed IM $S_{a,av}(T_1,T_e)$ with varying period band ΔT for a system with parameters as specified

3.2. Overall Dependence of the Dispersion on Characteristic Structural Parameters

Subsequently, the dependence of the collapse dispersion parameter s^* due to aleatory uncertainties on two predominant structural parameters of the considered SDOF systems is investigated. These parameters are the fundamental period T_1 and the negative post-yield stiffness ratio $\theta-\alpha$. The influence of the damping coefficient ζ, and of the shape of the hysteretic loop will be addressed in a future study.

For each considered structural configuration (T_1, $\theta-\alpha$) the collapse capacity is determined for all records of the ATC-63 FF ground motion set by IDA, and parameter s^* evaluated subsequently. This analysis is performed seven times varying the period band width ΔT (ΔT = 0 s, 0.4 s, 0.6 s, 0.8 s, 1.0 s, 1.2 s, 1.4 s) of the proposed IM $S_{a,av}(T_1,T_e)$ in an effort to identify the "optimal" period band ΔT with smallest dispersion s^* of the collapse capacity. The structural period T_1 is increased in steps in the range from 0.1 s to 5 s. For the parameter $\theta-\alpha$ the following discrete values are considered: $\theta-\alpha$ = 0.04, 0.06, 0.08, 0.10, 0.15, 0.20, 0.25, 0.30, 0.35, 0.40, 0.45, 0.50, 0.60, 0.80.

In particular, it is of interest to study the general trend of s^* for each period band ΔT with respect to the structural period T_1 and the negative post-yield stiffness ratio $\theta-\alpha$. Thus, at first for each period T_1 and each IM the mean value of s^* (denoted subsequently as $\overline{s}^*_{\theta-\alpha}$) from all outcomes comprising the entire set of parameters $\theta-\alpha$ is evaluated. In Fig. 3.3a $\overline{s}^*_{\theta-\alpha}$ is plotted against the period T_1 for each considered ΔT. The full line in blue corresponds to $\overline{s}^*_{\theta-\alpha}$ of the original base study of Adam and Jäger (2012a) using the conventional IM $S_a(T_1)$ (i.e. $\Delta T = 0$). For short period systems with T_1 = 0.1 s the traditional IM exhibits the best performance with respect to the smallest mean dispersion of the collapse capacity. In the subsequent range of periods (T_1 = 0.2 s to 0.4 s) $\overline{s}^*_{\theta-\alpha}$ is smallest for $S_{a,av}(T_1,T_e)$ with ΔT = 0.4 s. This trend continues, and finally the largest considered period band of ΔT = 1.4 s exhibits the smallest $\overline{s}^*_{\theta-\alpha}$ for flexible structures with periods larger than 1.7 s. The reduction rate of $\overline{s}^*_{\theta-\alpha}$ decreases with increasing ΔT and T_1. For example, the difference of $\overline{s}^*_{\theta-\alpha}$ based on ΔT = 1.4 s and on ΔT = 1.2 s, respectively, is almost negligible. From the result of Fig. 3.3a it can be concluded that there is no optimal IM for the entire range of structural periods, and thus, the IM should be a function of the structural period T_1. Furthermore, it has been revealed that for periods larger than 0.5 s the dispersion of the collapse capacity based on the conventional IM $S_a(T_1)$ is a maximum. Compared to the results based on $S_a(T_1)$ the enhanced IM $S_{a,av}(T_1,T_e)$ leads to the reduction of the mean collapse capacity dispersion up to 45%.

Next, the overall trend of the dispersion parameter s^* with respect to negative post-yield stiffness ratio $\theta-\alpha$ is studied. Fig. 3.3b shows the mean value of s^* (denoted as $\overline{s}^*_{T_1}$) with respect to all outcomes comprising the entire set of considered periods T_1 as a function of $\theta-\alpha$. In representation the

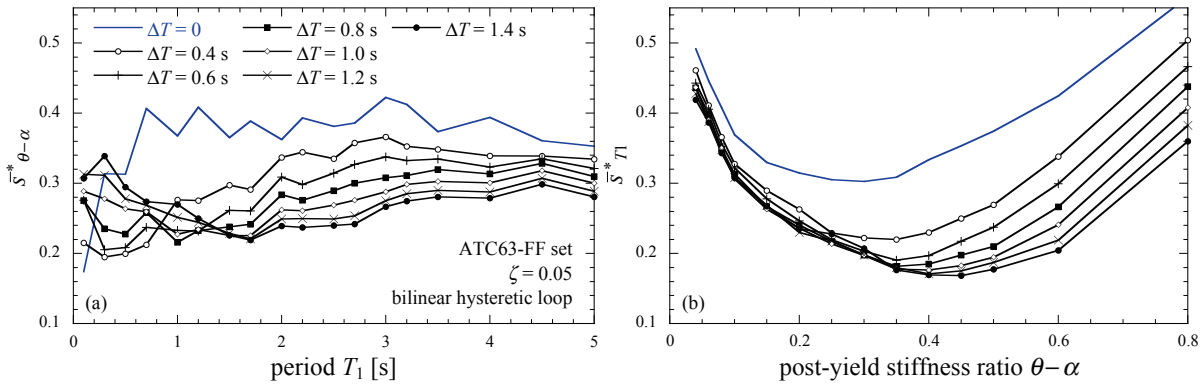

Figure 3.3. Mean values $\overline{s}^*$ of dispersion s^* determined from the individual dispersion of all collapse capacities taking into account (a) the whole range of considered post-yield stiffness ratios $\theta-\alpha$ at each period T_1, and (b) taking into account the whole range of considered periods T_1 for each ratio $\theta-\alpha$

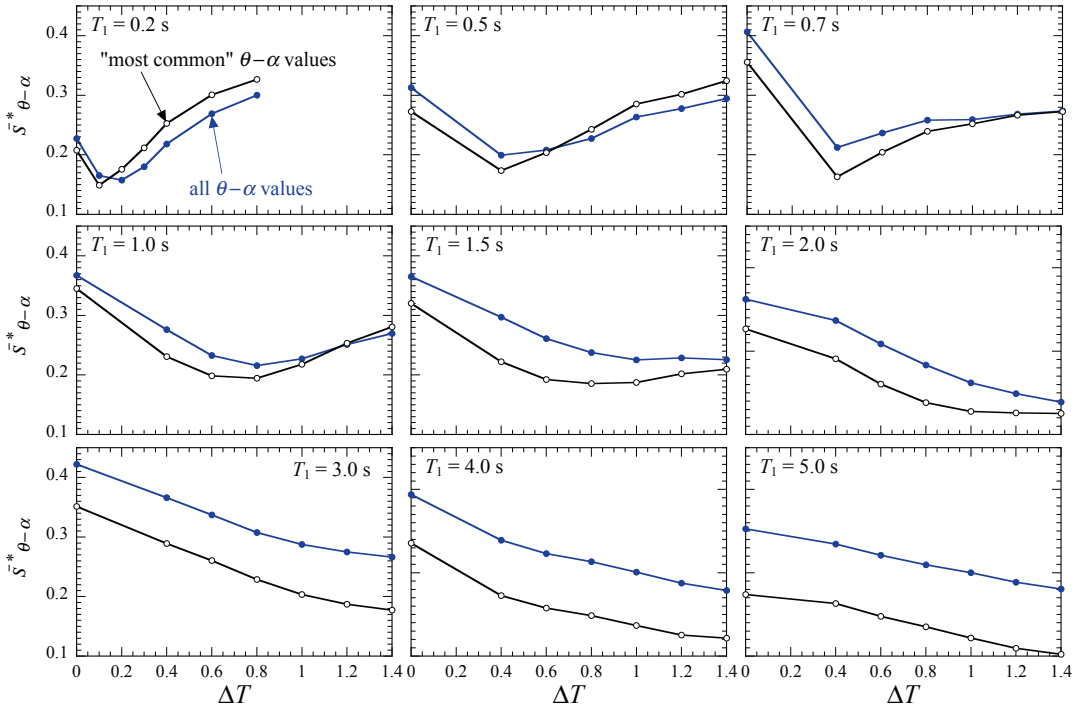

Figure 3.4. Mean dispersion $\bar{s}^*$ of the collapse capacities as a function of the period band ΔT in the proposed IM $S_{a,av}(T_1,T_e)$ for nine discrete periods T_1. Blue lines: mean taking into account all considered post-yield stiffness ratios. Black lines: mean taking into account post-yield stiffness ratios in the range of $0.10 \leq \theta-\alpha \leq 0.45$

performance is poorest in the entire parameter range $\theta-\alpha$ for the conventional IM $S_a(T_1)$. It is interesting to note that the dispersion is a minimum for moderate and large values of the post-yield stiffness ratio in the range of $\theta-\alpha = 0.30$ to 0.50. For mild and extreme values of $\theta-\alpha$ ($\theta-\alpha < 0.10$, $\theta-\alpha > 0.60$) the reduction of $\bar{s}^*_{T_1}$ with respect to the results for the IM $S_a(T_1)$ is less pronounced (Fig. 3.3b).

Fig. 3.4 shows for nine discrete structural periods T_1 the mean of the collapse capacity dispersion $\bar{s}^*_{\theta-\alpha}$ plotted against the period band ΔT of the underlying IM $S_{a,av}(T_1,T_e)$. Thereby, on the one hand the mean $\bar{s}^*_{\theta-\alpha}$ is determined for all systems comprising the entire set of considered post-yield stiffness ratios $\theta-\alpha$. These results are depicted in blue. On the other hand only the collapse capacities of the "most common" ratios $\theta-\alpha$ in the range $0.10 \leq \theta-\alpha \leq 0.45$ are used to calculate the mean dispersion $\bar{s}^*_{\theta-\alpha}$. Black lines show these outcomes. It is confirmed that the "optimal" period band width ΔT of the IM $S_{a,av}(T_1,T_e)$ depends strongly on the structural period T_1. In general, the optimal value of ΔT becomes larger with increasing period T_1. For example, for $T_1 = 0.50$ s a ΔT of 0.40 s leads to the minimum mean dispersion. In this case the reduction of $\bar{s}^*_{\theta-\alpha}$ is about 45% compared to its counterpart for $\Delta T = 0$. If $T_1 = 1.00$ s, the most efficient ΔT is about 0.8 s.

Fig. 3.5 shows the reduction of the mean dispersion $\bar{s}^*_{\theta-\alpha,T_1}$ in % based on the proposed IM $S_{a,av}(T_1,T_e)$ compared to the outcomes using $S_a(T_1)$. Fig. 3.5 provides in the first column the total reduction for relatively stiff systems ($0.2 \leq T_1 < 0.5$ s). The selected period band is $\Delta T = 0.2$ s. The proposed approach leads to a dispersion reduction of 23.7%. The further bars in red show the mean dispersion reduction for all structural configurations in the period intervals $0.5 \leq T_1 < 0.7$ s, $0.7 \leq T_1 < 1.5$ s, and $1.5 \leq T_1 < 5.0$ s, respectively, and the corresponding "optimal" period bands ΔT as denoted in the legend. Here, the reduction of $\bar{s}^*_{\theta-\alpha,T_1}$ increases up to 45.2% at best. Additionally, for flexible structures ($1.5 \leq T_1 < 5.0$ s) the decrease of $\bar{s}^*_{\theta-\alpha,T_1}$ for different band widths ΔT as listed is visualized.

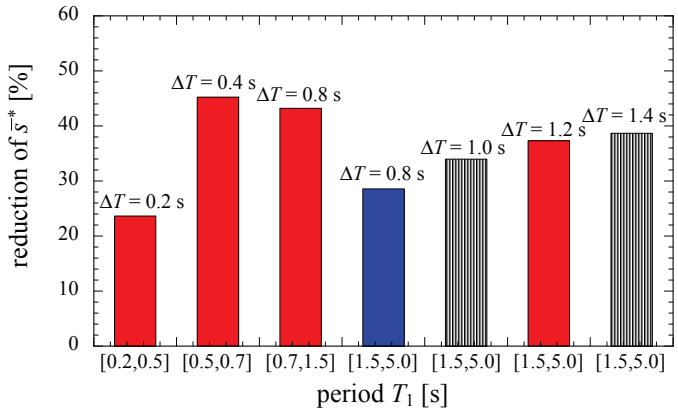

Figure 3.5. Reduction of the mean dispersion $\bar{s}^*$ of the collapse capacities based on the proposed IM $S_{a,av}(T_1,T_e)$ with respect to the ones based on the conventional IM $S_a(T_1)$ for different period ranges of T_1. Band width of averaging ΔT as specified. Post-yield stiffness ratios considered in the range $0.10 \le \theta - \alpha \le 0.45$

4. ENHANCED COLLAPSE CAPACITY SPECTRA

From the discussion above it can be concluded that it would be advantageous to select a period dependent band width $\Delta T = \Delta T(T_1)$ when the collapse capacity is based on the proposed IM $S_{a,av}(T_1,T_e)$. For stiff systems ($T_1 \le 0.2$ s) it is recommended to use the conventional IM $S_a(T_1)$. In the period range 0.2 s $\le T_1 \le$ 0.5 s the proposed band width ΔT is 0.2 s. For 0.5 s $\le T_1 \le$ 0.7 s the proposed band width ΔT increases to 0.4 s, then in the range 0.7 s $\le T_1 \le$ 1.5 s ΔT is 0.8 s, and for flexible structures 1.5 s $\le T_1 \le$ 5.0 s a ΔT of 1.2 s has been selected.

Fig. 4.1 shows improved median collapse capacity spectra for three selected post-yield stiffness ratios $\theta - \alpha$ = 0.10, 0.20, and 0.40. For each parameter $\theta - \alpha$, spectra based on the proposed period bands ΔT = 0 s, 0.2 s, 0.4 s, 0.8 s, and 1.2 s are depicted. Bold lines correspond to the recommended values of the median collapse capacities, depending on the period ranges T_1, and in most cases to the lowest envelops of the dispersion s^*, compare with Fig. 4.2. In Fig. 4.2 the dispersion parameter s^* is depicted for each considered ΔT, and $\theta - \alpha$ = 0.10, 0.20 and 0.40. Furthermore, it can be seen that for periods T_1 > 0.2 s the median collapse capacities become smaller with increasing ΔT. This is a result of "averaging" the spectral acceleration in the band width ΔT in the descending branch of this quantity.

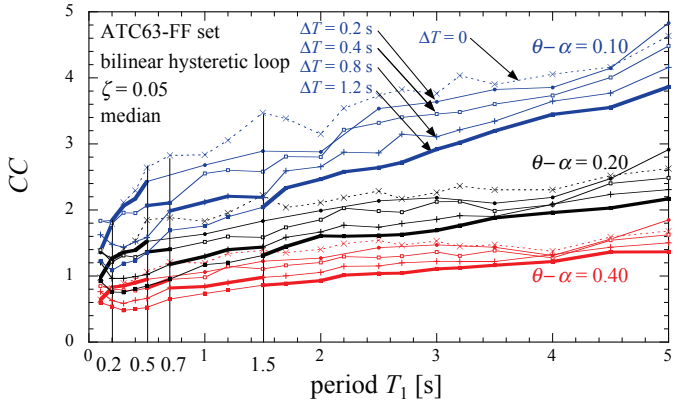

Figure 4.1. Improved median collapse capacity spectra for different averaging band width ΔT in the underlying IM $S_{a,av}(T_1,T_e)$. Bold lines: Period dependent sections of the proposed spectra

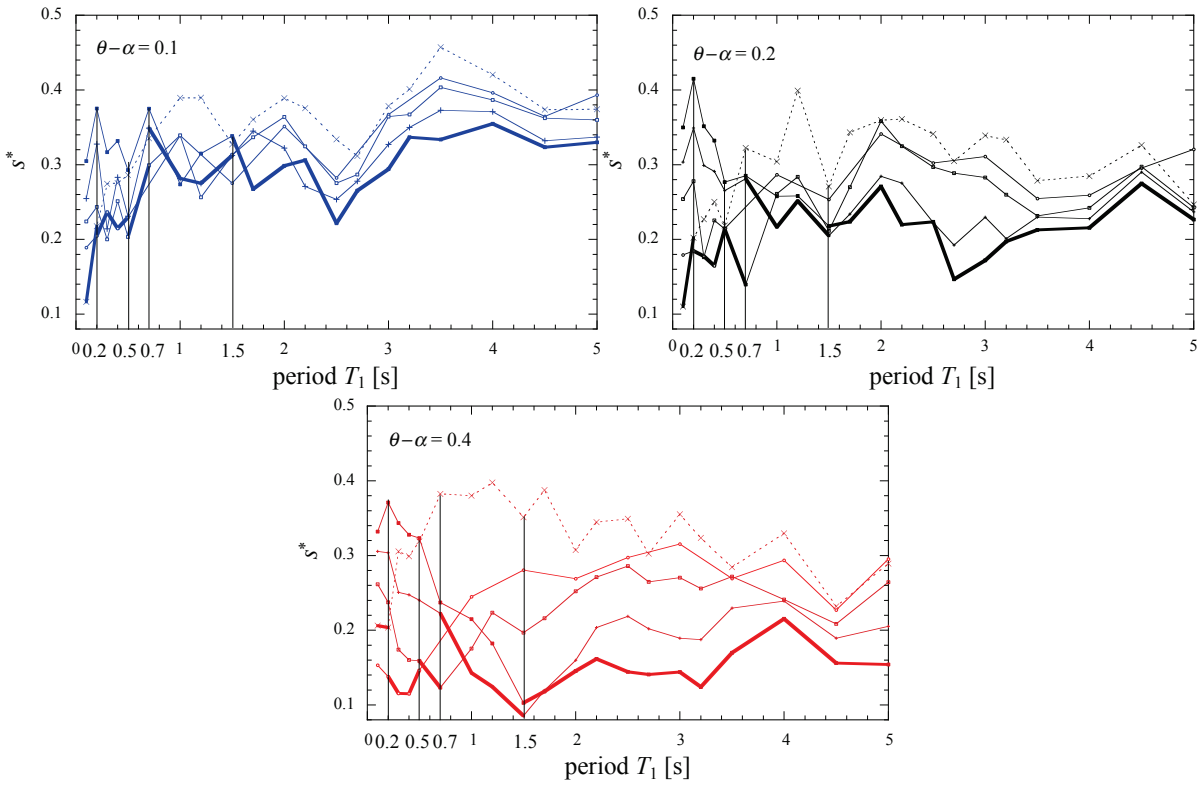

Figure 4.2. Dispersion parameter s^* of the improved collapse capacities for different averaging band width ΔT in the underlying IM $S_{a,av}(T_1,T_e)$. Three different post-yield stiffness ratios $\theta-\alpha$. Bold lines: Period dependent sections of the corresponding median collapse capacity spectra depicted in Figure 4.1

5. CONCLUSION

The use of an average spectral acceleration over a range of periods between the structural period and an elongated period as intensity measure (IM) leads to a substantial reduction of the record-to-record variability of the collapse capacity of inelastic non-deteriorating single-degree-of-freedom systems vulnerable to the P-delta effect. Based on this IM enhanced collapse capacity spectra were presented. In the applied approach the range of periods for averaging the spectral acceleration depends on the structural period. For almost rigid systems this period range is zero, and thus the proposed IM degenerates to the conventional one considering the spectral acceleration at a specific discrete period. The more flexible the system becomes the larger is the "optimal" period range for averaging the spectral acceleration. In a subsequent step nonlinear regression analyses will be applied to obtain analytical expressions for the mean collapse capacity spectra and its dispersion. The incorporation of the higher mode effect to the suggested IM can be proved only for multi-degree-of-freedom structures. The ultimate aim is the derivation of compact and accurate design collapse capacity spectra of flexible multi-story structures in order to establish a level of safety against second-order effects of gravity.

ACKNOWLEDGEMENT

The first author conducted the research for this paper as a student of the Doctoral School (FWF DK-plus) "Computational Interdisciplinary Modelling", which is based at the University of Innsbruck and substantially funded by the Austrian Science Fund (FWF). The investigations of the second author were partially funded by the Tyrolean Science Fund (TWF). This support is gratefully acknowledged.

REFERENCES

Adam, C. and Jäger, C. (2012a). Seismic collapse capacity of basic inelastic structures vulnerable to the P-delta effect. *Earthquake Engineering and Structural Dynamics* **41**, 775-793.

Adam, C. and Jäger, C. (2012b). Dynamic instabilities of simple inelastic structures subjected to earthquake excitation. *Advanced Dynamics and Model-Based Control of Structures and Machines* (Irschik, H., Krommer, M., Belyaev, A., eds), pp. 11 -18. Wien, New York: Springer.

Asimakopoulos, A.V., Karabalis, D.L. and Beskos, D.E. (2007). Inclusion of the P-Δ effect in displacement-based seismic design of steel moment resisting frames. *Earthquake Engineering and Structural Dynamics* **36**, 2171-2188.

ATC 40 (1996). Seismic Evaluation and Retrofit of existing concrete buildings. Applied Technology Council: Redwood City CA.

ATC 58 (2009). Guidelines for seismic performance assessment of buildings. ATC-58 50% Draft. Applied Technology Council: Redwood City CA.

Baker, J.W. (2007). Measuring bias in structural response caused by ground motion scaling. *8th Pacific Conference on Earthquake Engineering* (8PCEE 07), December 5-7, 2007, Nangyang Technological University: Singapore, 8 pp.

Baker, J.W. and Cornell, C.A. (2005). A vector-valued ground motion intensity measure consisting of spectral acceleration and epsilon. *Earthquake Engineering and Structural Dynamics* **34:10**, 1193-1217.

Bernal, D. (1987). Amplification factors for inelastic dynamic P-Δ effects in earthquake analysis. *Earthquake Engineering and Structural Dynamics* **15**, 635-651.

Baker J.W. and Jayaram, N. (2008). Correlation of spectral acceleration values from NGA ground motion models. *Earthquake Spectra* **24:1**, 299-317.

Bianchini, M., Diotallevi, P. and Baker, J.W. (2009). Prediction of inelastic structural response using an average of spectral accelerations. *10th International Conference on Structural Safety and Reliability* (ICOSSAR 09), September 13-19, 2009, Osaka, Japan, 8pp.

Deierlein, G.G. (2004). Overview of a comprehensive framework for earthquake performance assessment. *Performance-Based Seismic Design. Concepts and Implementation* (Fajfar, P. and Krawinkler H. eds). Proc. of the International Workshop, June 28-July 1, 2004, Bled, Slovenia, pp. 15-26.

FEMA 273 (1997). NEHRP quidelines for the seismic rehabilitation of buildings. Federal Emergency Management Agency: Washington D.C.

FEMA P-695 (2009). Quantification of Building Seismic Performance Factors. Federal Emergency Management Agency: Washington D.C.

Haselton, C.B. and Baker, J.W. (2006). Ground motion intensity measures for collapse capacity prediction: choice of optimal spectral period and effect of spectral shape. *8th National Conference on Earthquake Engineering*, San Francisco, California, April 18-22, 10 pp.

Ibarra, L.F. and Krawinkler, H. (2005). Global collapse of frame structures under seismic excitations. PEER 2005/06. Pacific Earthquake Engineering Research Center, University of California at Berkeley, California.

Ibarra, L. and Krawinkler, H. (2011). Variance of collapse capacity of SDOF systems under earthquake excitations. *Earthquake Engineering and Structural Dynamics* **40:12**, 1299-1314.

Kadas, K., Yakut,A. and Kazaz I. (2011). Spectral ground motion intensity based on capacity and period elongation.*Journal of Structural Engineering* **137:3**, 401-409.

Krawinkler, H., Zareian, F., Lignos, D.G. and Ibarra, L.F. (2009). Prediction of collapse of structures under earthquake excitations. *2nd International Conference on Computational Methods in Structural Dynamics and Earthquake Engineering*. (Papadrakakis M, Lagaros ND, Fragiadakis M. eds). June 22-24, 2009, Rhodes, Greece, CD-ROM paper, paper no. CD449.

Limpert, E., Stahel, W.A. and Abbt, M. (2001). Log-normal distributions across the sciences: Keys and clues. *BioScience* **51:5**, 341-352.

MacRae, G.A. (1994) P-Δ effects on single-degree-of-freedom structures in earthquakes. *Earthquake Spectra* **10**, 539-568.

Miranda, E. and Akkar, S.D. (2003). Dynamic instability of simple structural systems. *Journal of Structural Engineering* **129**, 1722-1726.

Tothong, P. and Luco, N. (2007). Probabilistic seismic demand analysis using advanced ground motion intensity measures. *Earthquake Engineering and Structural Dynamics* **36:13**, 1813-1860.

Vamvatsikos, D. and Cornell, C.A. (2002). Incremental dynamic analysis. *Earthquake Engineering and Structural Dynamics* **31**, 491-514.